Cervical cancer evaluated with integrated ^{18}F-FDG PET/MR

JING GONG[1,2*], NAN WANG[1*], LIHUA BIAN[1], MIN WANG[1], MINGXIA YE[1], NA WEN[1], MENG FU[3], WENSHENG FAN[1] and YUANGUANG MENG[1]

[1]Department of Obstetrics and Gynecology, Chinese PLA General Hospital, Beijing 100853; [2]Department of Obstetrics and Gynecology, Beijing Anzhen Hospital, Capital Medical University, Beijing 100029; [3]Department of Obstetrics and Gynecology, Haidian Maternal and Child Health Hospital, Beijing 100080, P.R. China

Received October 19, 2018; Accepted April 15, 2019

DOI: 10.3892/ol.2019.10514

Abstract. The current study aimed to evaluate the correlation between maximum standardized uptake value (SUV_{max}) and minimum apparent diffusion coefficient (ADC_{min}) of cervical cancer using an integrated ^{18}F-fluorodeoxyglucose positron emission tomography/magnetic resonance (PET/MR) imaging system, and to determine the association with pathological prognostic factors. A total of 46 patients were pathologically diagnosed with cervical cancer and underwent PET/MR prior to surgery, including total hysterectomy, bilateral pelvic lymph node dissection or paraaortic lymph node dissection. The imaging biomarkers included the SUV_{max} and $ADC_{min.}$ The pathological prognostic factors were as follows: Tumor size, histological grade, International Federation of Gynecology and Obstetrics (FIGO) stage and lymph node metastasis. Pearson's correlation analysis was used to evaluate the correlation between imaging biomarkers and the tumor size and the Mann-Whitney U test analysis was used to evaluate the association between imaging biomarkers and pathological factors. The mean SUV_{max} was 11.1±8.7 (range, 3.16-51.6) and the mean ADC_{min} was 0.76±0.15x10^{-3} mm^2/s (range, 0.47-1.04x10^{-3} mm^2/s). The SUV_{max} had a significant negative correlation with the ADC_{min} (r=-0.700; P<0.001). The SUV_{max} was significantly increased in patients with poorly differentiated tumors (P=0.001), patients with FIGO stage IIB (P=0.005) and the patients with lymph node metastasis (P=0.040). The ADC_{min} was significantly decreased in patients with poorly differentiated tumors (P<0.001) and patients with FIGO stage IIB (P=0.017). Statistical analysis revealed no significant correlation between the tumor size and the SUV_{max} (r=0.286;P=0.054), or between the tumor size and the ADC_{min} (r=-0.231; P=0.122). Area under the curve (AUC) analysis revealed that SUV_{max} had a higher diagnostic value for lymph node metastasis (AUC=0.681) and FIGO staging (AUC=0.837) compared with ADC_{min}, whereas ADC_{min} had a higher diagnostic value for the grade of pathological differentiation (AUC=0.816) compared with SUV_{max} (AUC=0.788). The results of the current study demonstrated that there was a significant negative correlation between SUV_{max} and ADC_{min}, which were associated with prognostic factors.

Correspondence to: Professor Yuanguang Meng or Professor Wensheng Fan, Department of Obstetrics and Gynecology, Chinese PLA General Hospital, 28 Fuxing Road, Beijing 100853, P.R. China
E-mail: meng6512@vip.sina.com
E-mail: fanws99@163.com

*Contributed equally

Abbreviations: SUV_{max}, maximum standardized uptake value; ADC_{min}, minimum apparent diffusion coefficient; ^{18}F-FDG, ^{18}F-fluorodeoxyglucose; PET/MR, positron emission tomography/magnetic resonance; AUC, area under the curve; FIGO, International Federation of Gynecology and Obstetrics; ROI, region of interest

Key words: maximum standardized uptake value, minimum apparent diffusion coefficient, cervical cancer, positron emission tomography/magnetic resonance imaging, histological grade, International Federation of Gynecology and Obstetrics stage, lymph node metastasis

Introduction

Cervical cancer is one of the most common gynecological cancers. In China, cervical cancer is the second most common cancer in females after breast cancer (1). In 2012, ~52,7600 new cases of cervical cancer were diagnosed worldwide and 265700 patients succumbed (2). The average age of diagnosis for cervical cancer is 50 years, which is younger than that of other types of cancer, including endometrial and ovarian cancers (3). Pretreatment evaluation of patients with cervical cancer, including staging and assessment of prognostic factors, is required for predicting the prognosis and determining the optimal treatment regimen (4).

Previous studies have revealed that patient age, clinical symptoms, degree of pathological differentiation, International Federation of Gynecology and Obstetrics (FIGO) stage, status of lymph node metastasis and tumor size affect the prognosis of patients with cervical cancer (5,6). Imaging diagnosis of cervical cancer may assist clinical decision making. Positron emission tomography (PET) and magnetic resonance (MR) imaging serve important roles in the diagnosis and treatment of tumors. Diffusion-weighted imaging (DWI) is an imaging method that reflects the diffusion of water molecules through the apparent diffusion coefficient (ADC), which is

negatively correlated with tumor cellularity. This method can reflect the diffusion limitation and molecular density of tumor tissue (7). It is frequently used in tumor diagnosis and prognosis evaluation (8). ^{18}F-fluorodeoxyglucose (^{18}F-FDG) PET reflects glucose metabolism of the tumor, as the faster the tumor cells proliferate, the higher their metabolic rate. Patients with cervical cancer manifest lesions with marked elevations in metabolic rate on PET images (9). The standardized uptake value (SUV) is used to measure the glucose uptake within a region of interest (ROI), and may be used to assess tumor aggressiveness and prognosis (10). The maximum SUV (SUV_{max}) may be used as an independent prognostic factor (11). SUV and ADC values are associated with a number of pathological prognostic factors and may be used to assess the prognosis of patients. The two aforementioned parameters may serve a complementary role in describing tumor characteristics and assessing the prognosis of cervical cancer. Unlike PET and MR imaging, integrated PET/MR imaging provides multiparametric functional images in a single examination, including a DWI (7). Additionally, ^{18}F-FDG PET/MR imaging provides metabolic information. PET/MR imaging provides comprehensive information about tumor characteristics, including the location, size and extent of the lesion (12,13). Furthermore, deviations caused by physiological changes during the time interval between PET and MR imaging are avoided (7). Previous studies have revealed that integrated PET/MR provides comprehensive information and excellent image quality in the diagnosis and staging of different types of cancers, and is superior to PET alone (14-16).

Previous studies have revealed that the maximum standard uptake value (SUV_{max}) has a negative correlation with the minimum ADC (ADC_{min}) on PET/MR imaging for various types of cancer, including endometrial (11), rectal (17), cervical (18) and breast cancer (19). However, there are currently few studies on the combination of DWI and PET functional imaging for the detection of cervical cancer (13,18). The aim of the current study was to evaluate the correlation between the SUV_{max} and the ADC_{min} using an integrated PET/MR imaging system, and to establish the correlation with pathological prognostic factors.

Materials and methods

Patients. This study was approved the Ethics Committee of the Chinese PLA General Hospital and all patients signed informed consent forms. Patients were enrolled in the Chinese PLA General Hospital (Beijing, China) between April 2016 and December 2017, and follow up was conducted one time six months following surgery. All patients had undergone PET/MR imaging examinations prior to surgery, including total hysterectomy, bilateral pelvic lymph node dissection and paraaortic lymph node dissection. A total of 46 patients were pathologically confirmed to have cervical cancer (mean age, 56.5±12.1; range, 31-74). The inclusion criteria were as follows: i) Clinical suspicion of cervical cancer; and ii) histopathological diagnosis of cervical cancer following PET/MR imaging. The exclusion criteria were as follows: i) Pregnant patients; ii) patients with metal implants; iii) patients with claustrophobia, iv) patients with impaired renal function; and v) patients with poor quality PET/MR images.

Table I. Clinical data of the 46 patients with cervical cancer in the present study.

Characteristics	Value
Age (years)	56.5±12.1 (31-74)
Tumor size (mm^3)	10.3±9.8 (0.72-60)
Histology	
Adenocarcinoma	6 (13)
Squamous carcinoma	40 (87)
Histology grade	
Well-differentiated	0 (0)
Moderately-differentiated	23 (50)
Poorly-differentiated	23 (50)
International Federation of Gynecology and Obstetrics stage	
IB	25 (54)
IIA	10 (22)
IIB	11 (24)
Lymph node metastasis	
Absent	28 (61)
Present	18 (39)

The data are presented as the mean ± standard deviation (range) or number (percentage) of patients.

Following tumor resection, tissues were fixed with 10% formaldehyde for 24 h, dehydrated in an ethanol gradient (100, 95, 85 and 75% ethanol for 5, 4, 3 and 2 min, respectively), wax-impregnated and embedded in paraffin. Serial sections (5 μm thick) were prepared and dried at 50˚C for 30 min. Sections were stained with hematoxylin for 5 min and 1% eosin for 30-60 sec at room temperature. Histopathological evaluations of these sections were assessed using a light microscope (magnification, 40x). The patients received surgical treatment and the tumor size, grade, stage and the status of lymph node metastasis were recorded. The histopathologic findings were reviewed as previously described (20,21).

PET/MR examination. Whole-body PET/MR examination was performed using an integrated PET/MR machine (Biograph mMR; Siemens Healthineers). Prior to the examination, patients fasted for >6 h, and their fasting blood glucose levels were monitored. Prior to image acquisition, ^{18}F-FDG (Sumitomo HM-20 Cyclotron) 2.22-4.44 MBq/kg was injected intravenously at rest. Images were acquired 50-60 min following injection. The acquisition time was 3 min per bed position, and the accumulated acquisition time was 40 min/person. The attenuation correction technique was used based on the Dixon sequence: Images were reconstructed with an iterative algorithm (3 iterations; 21 subsets; and a Gaussian filter with a full width at half maximum=4 mm for scatter correction) incorporating a point spread function (22). MR image C was acquired using the complete Matrix coils to cover most of the trunk (from the neck to the middle segment of the femur). The sequences included 3D volumetric interpolated breath-hold T1-weighted sequence in the horizontal axis, and the

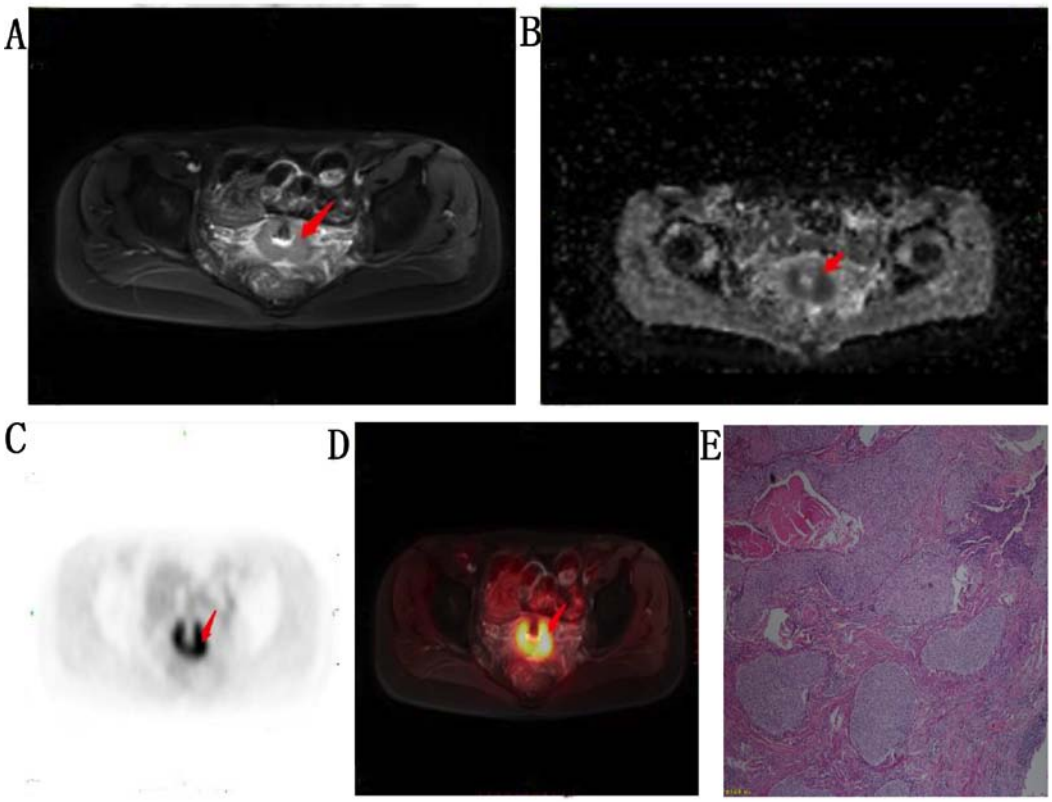

Figure 1. PET/MR scans of a 55 years old patient with cervical cancer (moderately differentiated, stage IB). (A) Axial T2-weighted MR image revealed a cervical tumor (red arrow). (B) An ADC map revealed low signal intensity of the tumor (red arrow; ADC_{min}=0.78x10^{-3} mm^2/s). (C) PET and (D) PET/MR hybrid images image revealed the high glucose metabolic activity of the tumor (red arrow; SUV_{max}=8.8). (E) Pathological images revealed moderate differentiation (magnification, 40x). PET, positron emission tomography; MR, magnetic resonance; ADC, apparent diffusion coefficient; min, minimum; SUV_{max}, maximum standardized uptake value.

T2-weighted turbo spin-echo imaging (T2WI-TSE) sequence in the horizontal axis. DWI with b values of 50 and 800 in the horizontal axis was performed. Patients with cervical cancer were scanned with the sagittal T2WI-TSE sequence.

Image analysis. Two nuclear medicine physicians independently measured the ADC_{min} and SUV_{max} of primary tumors. For the ADC value, the large ROIs were drawn manually to cover the lesions (with abnormal enhancement) on the DWI. The lowest ADC value was defined as the ADC_{min}. The ROI was manually delineated by the substantial part of abnormal enhancement within the lesion on the PET image, and syngo MMWP software (version VE40A; Siemens Healthineers) automatically calculated the SUV value of the lesion. The highest SUV value of the ROI was defined as the SUV_{max}.

Data analysis. All data were analyzed using SPSS software (version 19.0; IBM Corp., Armonk, NY, USA). Continuous data were presented as the mean ± standard deviation. Pearson's correlation analysis was used to evaluate the correlation between imaging biomarkers and the tumor size. The Mann-Whitney U test was used to evaluate the associations between the imaging biomarkers (SUV_{max} and ADC_{min}) and pathological factors (histological grade, FIGO stage and lymph node metastasis) (18,23). The sensitivity and specificity of the imaging biomarkers for pathological factors were determined by measuring the area under the curve (AUC). $P<0.05$ was considered to indicate a statistically significant difference.

Results

Patient clinical data. This study enrolled a total of 46 patients with a definitive pathological diagnosis of cervical cancer. The patients had a mean age of 56.5±12.1 years (range, 31-74). Detailed clinical data of the patients are presented in Table I. A total of 40 patients had squamous carcinoma and 6 had adenocarcinoma. A total of 23 patients had poorly differentiated carcinoma, 23 had moderately differentiated carcinoma and none had well differentiated carcinoma. The mean tumor size was 10.3±9.8 mm^3 (maximum size, 60 mm^3). All 46 patients underwent FIGO staging, which revealed stage IB in 25 patients (moderately differentiated; Fig. 1), stage IIA in 10 patients (moderately differentiated; Fig. 2) and stage IIB in 11 patients. A total of 18 patients had cervical invasion with lymph node metastasis, including left pelvic lymph node metastasis (poorly differentiated; stage IIA; Fig. 3) and bilateral pelvic lymph node metastasis (poorly differentiated; stage IIB; Fig. 4).

Analysis of the correlations between SUV_{max}, ADC_{min} and the tumor size. Following integrated PET/MR imaging for the 46 patients, the mean SUV_{max} was 11.1±8.7 (range, 3.16-51.6) and the mean ADC_{min} was 0.76±0.15x10^{-3} mm^2/s (range, 0.47-1.04x10^{-3} mm^2/s). The SUV_{max} had a significant negative correlation with the ADC_{min} (r=-0.700; P=<0.001; Fig. 5A). Statistical analysis revealed no significant difference between the tumor size and the SUV_{max} (r=0.286; P=0.054), or between

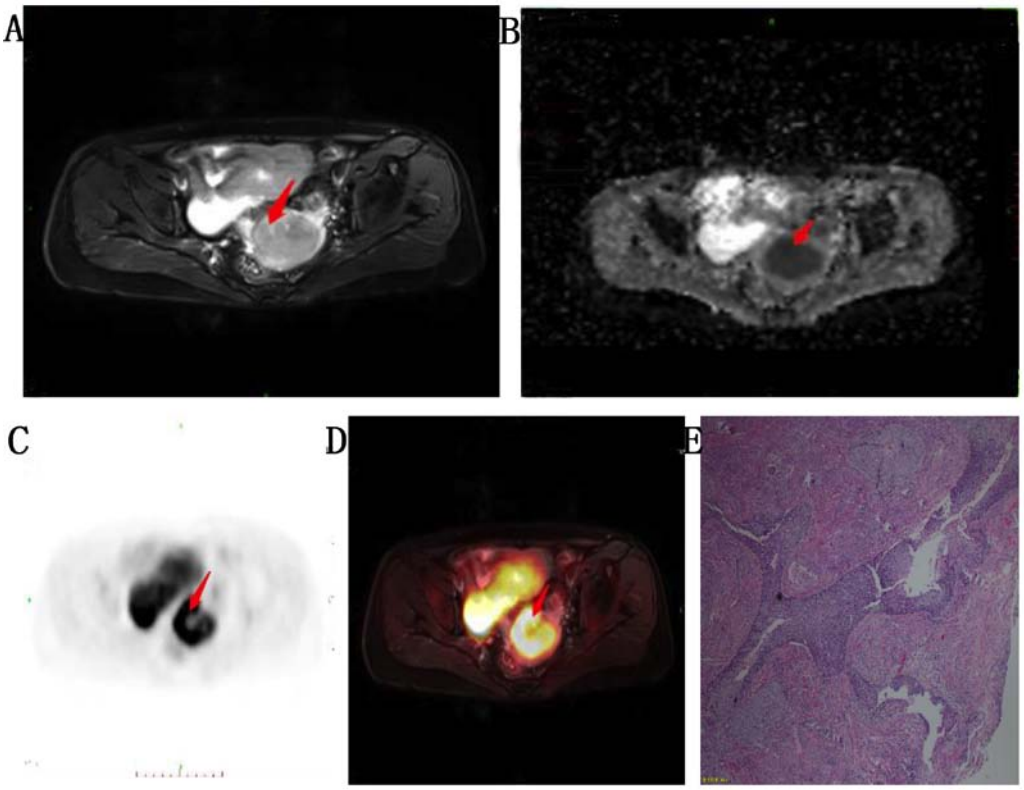

Figure 2. PET/MR scans of a 74 years old patient with cervical cancer (moderately differentiated, stage IIA). (A) Axial T2-weighted MR image revealed a cervical tumor (red arrow). (B) ADC map revealed the low signal intensity of the tumor (red arrow; ADC_{min}=0.63x10^{-3} mm^2/s). (C) PET and (D) PET/MR hybrid images revealed the high glucose metabolic activity of the tumor (red arrow; SUV_{max}=15.6). (E) Pathological images revealed moderate differentiation (magnification, x40). PET, positron emission tomography; MR, magnetic resonance; ADC, apparent diffusion coefficient; min, minimum; SUV_{max}, maximum standardized uptake value.

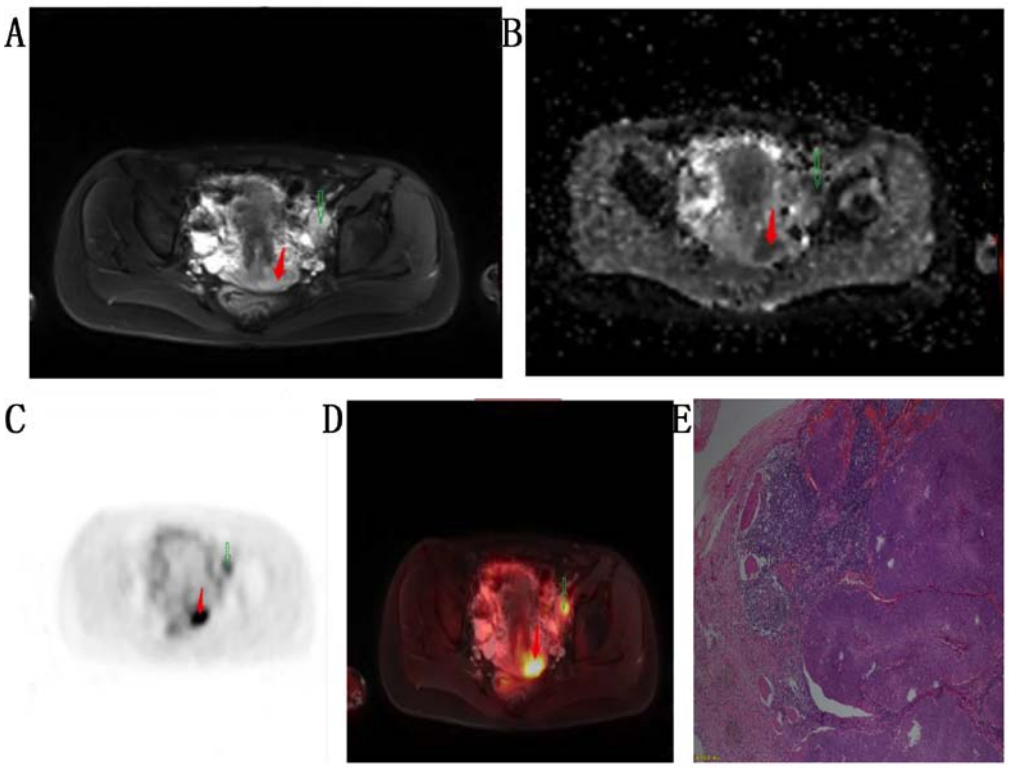

Figure 3. PET/MR scans of a 45 years old female with cervical cancer (poorly differentiated, stage IIA). (A) Axial T2-weighted MR image revealed a primary tumor (red arrow) and a secondary tumor (hollow arrow) in the left pelvic cavity. (B) ADC map revealed the low signal intensity of the tumor (red arrow; primary tumor ADC_{min}=0.8x10^{-3} mm^2/s). (C) PET and (D) PET/MR hybrid images image revealed the high glucose metabolic activity of the tumor (red arrow; primary tumor SUV_{max}=9). (E) Pathological images revealed shows poorly differentiation (magnification, x40). PET, positron emission tomography; MR, magnetic resonance; ADC, apparent diffusion coefficient; min, minimum; SUV_{max}, maximum standardized uptake value.

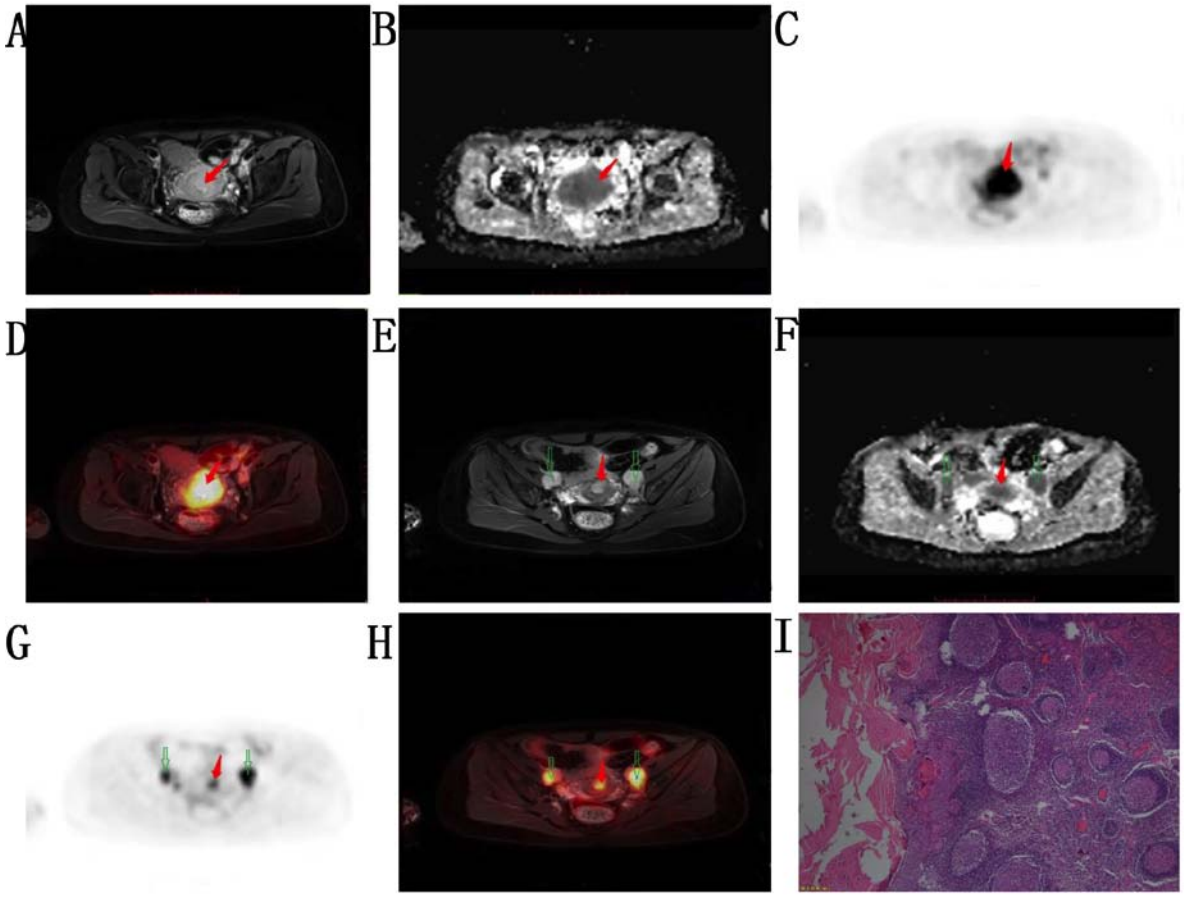

Figure 4. PET/MR scans of a 49 years old female with cervical cancer (poorly differentiated, stage IIB). (A) Axial T2-weighted MR image revealed a tumor (red arrow). (B) ADC map revealed low signal intensity of the tumor (red arrow; primary tumor ADC_{min}=0.67x10^{-3} mm^2/s). (C) PET and (D) PET/MR hybrid images revealed high glucose metabolic activity of the tumor (red arrow; primary tumor SUV_{max}=16.3). (E) Axial T2-weighted MR image revealed the tumor in the cervix (arrow) with two metastatic lymph nodes (hollow arrow) in the right and left pelvic cavity. (F) ADC map revealed low signal intensity of the primary (red arrow) and metastatic (hollow arrow) lesions. (G) PET and (H) PET/MR hybrid images revealed high glucose metabolic activity of the tumor. (I) Pathological images revealed poor differentiation (magnification, x40). PET, positron emission tomography; MR, magnetic resonance; ADC, apparent diffusion coefficient; min, minimum; SUV_{max}, maximum standardized uptake value.

the tumor size and the ADC_{min} (r=-0.231; P=0.122). The results of correlation analyses are detailed in Table II.

Association between SUV_{max}/ADC_{min}/tumor size and tumor differentiation/FIGO stage/lymph node metastasis. The SUV_{max} was significantly increased in patients with poorly differentiated tumors (P=0.001), patients with lymph node metastasis (P=0.040) and patients with FIGO stage IIB (P=0.005) compared with patients with moderately differentiated tumors, patients with no lymph node metastasis and patients with early-stage (IB-IIA), respectively. The ADC_{min} was significantly decreased in patients with poorly differentiated tumors (P<0.001) and patients with FIGO stage IIB (P=0.017), compared with patients with moderately differentiated tumors and patients with FIGO stage IB-IIA, respectively. The ADC_{min} was decreased in patients with lymph node metastasis compared with those without lymph node metastasis, but the difference was not statistically significant (P=0.105). The tumor sizes were slightly larger in patients with poorly differentiated tumors (P=0.553), patients with FIGO stage IIB (P=0.193), and patients with lymph node metastasis (P=0.386), compared with patients with moderately differentiated tumors, FIGO stage IB-IIA and without lymph node metastasis, respectively, but the differences were not statistically significant (Table III).

Sensitivity and specificity of SUV_{max} and ADC_{min} for histological grade, FIGO stage and lymph node metastasis are presented in Fig. 5. SUV_{max} exhibited a higher AUC value for predicting FIGO stage (AUC=0.837) and lymph node metastasis (AUC=0.681) compared with ADC_{min} for predicting FIGO stage (AUC=0.745) and lymph node metastasis (AUC=0.643). ADC_{min} was more useful for predicting the grade of tumor differentiation (AUC=0.816) compared with SUV_{max} (AUC=0.788).

Discussion

The present study demonstrated that PET/MR imaging provides valuable imaging data for patients with cervical cancer. These PET/MR results were associated with various pathological factors and may serve a role in the evaluation of the prognosis of patients with cervical cancer. The SUV represents the metabolism of glucose in tumor cells (15,23).

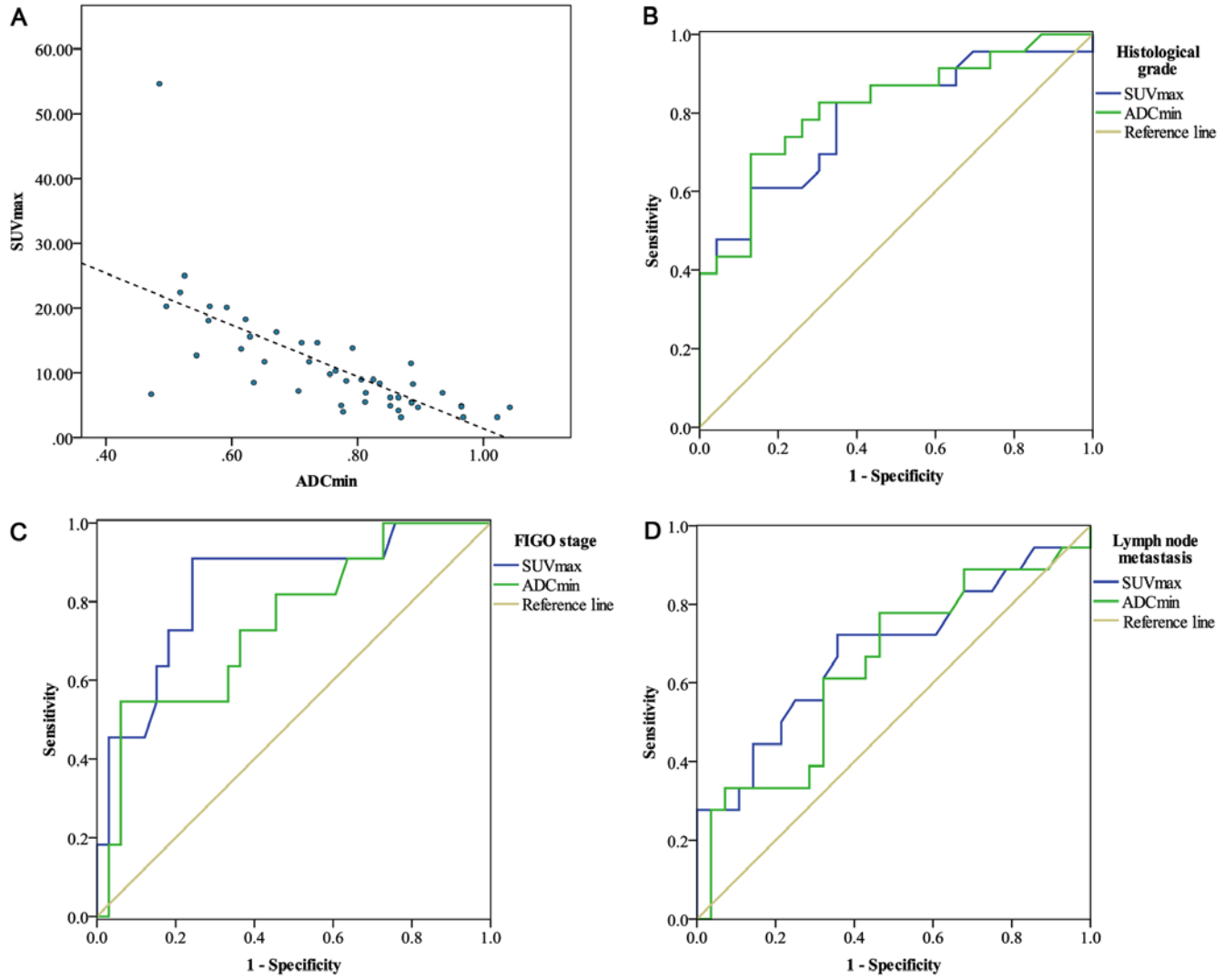

Figure 5. Correlation between ADC_{min} and SUV_{max} values of cervical cancer assessed by hybrid PET/MR and ROC to evaluate the diagnostic value of SUV_{max} and ADC_{min}. (A) A scatter plot revealed a significant inverse correlation between ADC_{min} and SUV_{max} (r=-0.700; P=<0.001). ROC to evaluate the diagnostic value of SUV_{max} and ADC_{min} in pathological prognostic factors in 46 patients with cervical cancer, including (B) histological grade, (C) FIGO stage and (D) lymph node metastasis. ADC_{min}, minimum apparent diffusion coefficient; SUV_{max}, maximum standardized uptake value; ROC, receiver operating characteristic curve; PET, positron emission tomography; MR, magnetic resonance; min, minimum; FIGO, International Federation of Gynecology and Obstetrics.

Table II. Correlations between SUV_{max}, ADC_{min} and tumor size.

Parameter	SUV_{max}	ADC_{min}	Tumor size
SUV_{max}			
r	1	-0.700	0.286
P-value		<0.001	0.054
ADC_{min}			
r		1	-0.231
P-value			0.122
Tumor size			
r			1
P-value			

SUV_{max}, maximum standardized uptake value; ADC_{min}, minimum apparent diffusion coefficient; r, Pearson product-moment correlation coefficient.

The invasive ability of tumors may be estimated from the SUV, and this may be used to predict the prognosis to some extent (24). The ADC presents tumor cellularity and may reflect tumor invasiveness (25). The ADC may be used to indicate tumor characteristics, including tumor size, number of metastatic lymph nodes, portal vein invasion and extrapancreatic nerve plexus invasion (25). Previous studies have revealed that the SUV_{max} and the ADC_{min} may be used as tumor imaging biomarkers, and they have a significantly negative correlation in different types of cancer, including endometrial (11), rectal (17), cervical (18) and breast cancer (19). As was the case with the aforementioned studies, the current study demonstrated that the SUV_{max} and the ADC_{min} had a significantly negative correlation, which may present a biological association between tumor cellularity and glucose metabolic activity. Previous studies relied on SUV and ADC values measured separately by distinct PET and MR devices (19,23). The time interval between the two examinations may impact the analysis. By contrast, an

Table III. Correlation between the SUV_{max}/ADC_{min}/tumor size and tumor differentiation/FIGO stage/lymph node metastasis.

	Histological grade			FIGO stage			Lymph node metastasis		
Parameter	Poorly differentiated (n =23)	Moderately differentiated (n =23)	P-value	(IB-IIA) (n=35)	IIB (n=11)	P-value	Absent (n=28)	Present (n=18)	P-value
SUV_{max}	14.9±10.6 (3.16-54.6)	7.3±3.6 (3.18-15.6)	0.001[a]	8.6±4.9 (3.16-22.4)	18.9±13.1 (4.94-54.6)	0.005	8.79±4.83 (3.18-20.1)	14.7±11.9 (3.16-54.)	0.040
ADC_{min} ($x10^{-3}$ mm^2/s)	0.67±0.14 (0.47-0.97)	0.84±0.11 (0.62-1.04)	0.000[a]	0.79±0.14 (0.47-1.04)	0.66±0.15 (0.48-0.97)	0.017	0.78±0.14 (0.47-1.02)	0.72±0.17 (0.48-1.04)	0.105
Tumor size (mm^3)	11.6±12.2 (2.89-60.0)	9.0±6.7 (0.72-25.0)	0.553	9.6±10.4 (0.72-60)	12.5±7.9 (2.89-25)	0.193	8.61±5.96 (3.0-25)	12.9±13.7 (0.72-60.0)	0.386

The data are presented as the means ± standard deviation (range). SUV_{max}, maximum standardized uptake value; ADC_{min}, minimum apparent diffusion coefficient; FIGO, International Federation of Gynecology and Obstetrics.

integrated PET/MR system provides the two types of data at the same time (26). The current study revealed that the SUV_{max} and the ADC_{min} had no significant correlation with the tumor size, as did a previous study by Kidd *et al* (27). Notably, a P-value close to 0.05 was obtained (P=0.054), and this warrants further investigation by expanding the sample size in future studies, as it may be used for guiding clinical diagnosis.

The grade of pathological differentiation and the FIGO stage are key factors affecting prognosis of patients with cervical cancer (28). The SUV_{max} and ADC_{min} are associated with pathological prognostic factors in various types of cancer (11,17,25). Previous studies revealed that tumor FDG uptake was associated with the grade of pathological differentiation: Poorly differentiated tumors had a higher SUV_{max} than moderately and well differentiated tumors (9,19,23,27). A previous study revealed that patients with poorly differentiated tumors had a decreased ADC compared with patients with well differentiated tumors (29). In addition, a previous study revealed that the SUV was positively correlated with the FIGO stage (4). The current study revealed a significantly increase in the SUV_{max} and a significant decrease in the ADC value in patients with poorly differentiated tumors compared with those with moderately differentiated tumors, as well as significant differences in the SUV_{max} and ADC_{min} values between patients with early cervical cancer (stage IB-IIA) and patients with mid-stage cervical cancer (stage IIB). The SUV in patients with stage (IIB-IIA) was decreased compared with patients with stage IIB. These results may be due to an increase in glucose uptake caused by the rapid growth and active proliferation of tumors, resulting in an increased FDG uptake in patients with poorly differentiated tumors.

The presence or absence of lymph node metastasis is an important prognostic factor in patients with early cervical cancer (9). Previous studies revealed SUV is significantly associated with lymph node metastasis (6,30). A previous study revealed that patients with cervical cancer with lymph node metastasis, had an increased SUV in their primary lesions compared with patients without lymph node metastasis (31). The current study demonstrated that a higher SUV was positively associated with lymph node metastasis, which indicated that high FDG uptake may predict local invasion of tumor cells. There was no significant difference in ADC_{min} between patients with lymph node metastasis and those without lymph node metastasis in the current study, contrary to observations made by Chen *et al* (32), who demonstrated that patients with lymph node metastasis had a significantly decreased ADC_{min} compared with patients without lymph node metastasis. This difference may be attributed to a smaller sample size.

Surgery is the preferred treatment for patients with early cervical cancer (4,13). By analyzing imaging markers to evaluate prognostic factors, surgical approaches may be optimized for individual patients (31,33). The current study demonstrated that PET had a higher diagnostic value for lymph node metastasis and FIGO staging than MR imaging alone, whereas MR imaging had a higher diagnostics value for the grade of pathological differentiation compared with PET. Thus, the comprehensive image data provided by an integrated PET/MR imaging system may have greater clinical significance than the data provided by MR imaging or PET alone.

There are two limitations for the current retrospective study. Firstly, no analysis was performed for the cervical cancer based on the pathological types due to the small sample size and future studies with a larger sample are required. Secondly, due to short follow-up time subsequent to the examination the postoperative survival of the patients was not included in the current study. The prognostic significance of the SUV and ADC were therefore not demonstrated.

In conclusion, the results of the current study revealed that there was a significant negative correlation between SUV_{max} and ADC_{min}. These two imaging biomarkers were associated with pathological prognostic factors. Compared with PET or MR imaging alone, integrated PET/MR imaging may provide higher value data for the diagnosis of cervical cancer.

Acknowledgements

Not applicable.

Funding

No funding was received.

Availability of data and materials

The datasets used and/or analyzed during the present study are available from the corresponding author on reasonable request.

Authors' contributions

JG and NWa designed the study and drafted the manuscript. WF and YM participated in the design of the study and provided guidance. MY performed the imaging examinations. NWa and MF collected the patient data. NWe, MF, LB and MW analyzed the data.

Ethics approval and consent to participate

The present study was approved by the Ethics Committee of Chinese PLA General Hospital and study participants provided written informed consent.

Patient consent for publication

Study participants provided their consent for the publication of data. All identifying patient data and images were removed.

Competing interests

The authors declare that they have no competing interests.

References

1. Chen W, Zheng R, Baade PD, Zhang S, Zeng H, Bray F, Jemal A, Yu XQ and He J: Cancer statistics in China, 2015. CA Cancer J Clin 66: 115-132, 2016.
2. Torre LA, Bray F, Siegel RL, Ferlay J, Lortet-Tieulent J and Jemal A: Global cancer statistics, 2012. CA Cancer J Clin 65: 87-108, 2015.
3. Petry KU: HPV and cervical cancer. In: HPV and cervical cancer. Springer, Berlin, Germany, pp59-62, 2012.
4. Bhatla N, Aoki D, Sharma DN and Sankaranarayanan R: Cancer of the cervix uteri. Int J Gynaecol Obstet 2 (Suppl 143): S22-S36, 2018.
5. Khiewvan B, Torigian DA, Emamzadehfard S, Paydary K, Salavati A, Houshmand S, Shamchi SP, Werner TJ, Aydin A, Roy SG, *et al*: Update of the role of PET/CT and PET/MRI in the management of patients with cervical cancer. Hell J Nucl Med 19: 254-268, 2016.
6. Tangjitgamol S, Anderson BO, See HT, Lertbutsayanukul C, Sirisabya N, Manchana T, Ilancheran A, Lee KM, Lim SE, Chia YN, *et al*: Management of endometrial cancer in Asia: Consensus statement from the asian oncology summit 2009. Lancet Oncol 10: 1119-1127, 2009.
7. Huellner MW, Appenzeller P, Kuhn FP, Husmann L, Pietsch CM, Burger IA, Porto M, Delso G, von Schulthess GK and Veit-Haibach P: Whole-body nonenhanced PET/MR versus PET/CT in the staging and restaging of cancers: Preliminary observations. Radiology 273: 859-869, 2014.
8. Preda L, Conte G, Bonello L, Giannitto C, Travaini LL, Raimondi S, Summers PE, Mohssen A, Alterio D, Cossu Rocca M, *et al*: Combining standardized uptake value of FDG-PET and apparent diffusion coefficient of DW-MRI improves risk stratification in head and neck squamous cell carcinoma. Eur Radiol 26: 4432-4441, 2016.
9. Viswanathan C, Faria S, Devine C, Patnana M, Sagebiel T, Iyer RB and Bhosale PR: [18F]-2-Fluoro-2-Deoxy-D-glucose -PET assessment of cervical cancer. PET Clin 13: 165-177, 2018.
10. Grant P, Sakellis C and Jacene HA: Gynecologic Oncologic Imaging With PET/CT. Semin Nucl Med 44: 461-478, 2014.
11. Nakamura K, Joja I, Fukushima C, Haruma T, Hayashi C, Kusumoto T, Seki N, Hongo A and Hiramatsu Y: The preoperative SUV_{max} is superior to ADC_{min} of the primary tumour as a predictor of disease recurrence and survival in patients with endometrial cancer. Eur J Nucl Med Mol Imaging 40: 52-60, 2013.
12. Collins CD: PET/CT in oncology: For which tumours is it the reference standard? Cancer Imaging 7 Spec No A: S77-S87, 2007.
13. Ashwin KR and Somashekhar SP: Management of early stage cervical cancer. Rev Recent Clin Trials 10: 302-308, 2015.
14. Kjær A, Loft A, Law I, Berthelsen AK, Borgwardt L, Löfgren J, Johnbeck CB, Hansen AE, Keller S, Holm S and Højgaard L: PET/MRI in cancer patients: First experiences and vision from copenhagen. MAGMA 26: 37-47, 2013.
15. Platzek I, Beuthien-Baumann B, Langner J, Popp M, Schramm G, Ordemann R, Laniado M, Kotzerke J and van den Hoff J: PET/MR for therapy response evaluation in malignant lymphoma: Initial experience. MAGMA 26: 49-55, 2013.
16. Drzezga A, Souvatzoglou M, Eiber M, Beer AJ, Fürst S, Martinez-Möller A, Nekolla SG, Ziegler S, Ganter C, Rummeny EJ and Schwaiger M: First clinical experience with integrated whole-body PET/MR: Comparison to PET/CT in patients with oncologic diagnoses. J Nucl Med 53: 845-855, 2012.
17. Er HÇ, Erden A, Küçük NÖ and Geçim E: Correlation of minimum apparent diffusion coefficient with maximum standardized uptake on fluorodeoxyglucose PET-CT in patients with rectal adenocarcinoma. Diagn Interv Radiol 20: 105-109, 2014.
18. Grueneisen J, Beiderwellen K, Heusch P, Buderath P, Aktas B, Gratz M, Forsting M, Lauenstein T, Ruhlmann V and Umutlu L: Correlation of standardized uptake value and apparent diffusion coefficient in integrated whole-body PET/MRI of primary and recurrent cervical cancer. PLoS One 9: e96751, 2014.
19. Baba S, Isoda T, Maruoka Y, Kitamura Y, Sasaki M, Yoshida T and Honda H: Diagnostic and prognostic value of pretreatment SUV in 18F-FDG/PET in breast cancer: Comparison with apparent diffusion coefficient from diffusion-weighted MR imaging. J Nucl Med 55: 736-742, 2014.
20. Kurman RJ, Carcangiu ML, Herrington CS and Young RH: WHO classification of tumours of female reproductive organs. 4th edition. IARC, Lyon, 2014.
21. Stock RJ, Zaino R, Bundy BN, Askin FB, Woodward J, Fetter B, Paulson JA, DiSaia PJ and Stehman FB: Evaluation and comparison of histopathologic grading systems of epithelial carcinoma of the uterine cervix: Gynecologic Oncology Group studies. Int J Gynecol Pathol 13: 99-108, 1994.
22. Martinez-Möller A, Eiber M, Nekolla SG, Souvatzoglou M, Drzezga A, Ziegler S, Rummeny EJ, Schwaiger M and Beer AJ: Workflow and scan protocol considerations for integrated whole-body PET/MRI in oncology. J Nucl Med 53: 1415-1426, 2012.
23. Shih IL, Yen RF, Chen CA, Chen BB, Wei SY, Chang WC, Sheu BC, Cheng WF, Tseng YH, Chen XJ, *et al*: Standardized uptake value and apparent diffusion coefficient of endometrial cancer evaluated with integrated whole-body PET/MR: Correlation with pathological prognostic factors. J Magn Reson Imaging 42: 1723-1732, 2015.
24. Chung HH, Nam BH, Kim JW, Kang KW, Park NH, Song YS, Chung JK and Kang SB: Preoperative [^{18}F]FDG PET/CT maximum standardized uptake value predicts recurrence of uterine cervical cancer. Eur J Nucl Med Mol Imaging 37: 1467-1473, 2010.
25. Hayano K, Miura F, Amano H, Toyota N, Wada K, Kato K, Sano K, Takeshita K, Aoyagi T, Shuto K, *et al*: Correlation of apparent diffusion coefficientmeasured by diffusionweighted MRI and clinicopathologic features in pancreatic cancer patients. J Hepatobiliary Pancreat Sci 20: 243-248, 2013.
26. Small W Jr, Strauss JB, Jhingran A, Yashar CM, Cardenes HR, Erickson-Wittmann BA, Gullett N, Kidd E, Lee LJ, Mayr NA, *et al*: ACR Appropriateness Criteria® definitive therapy for early-stage cervical cancer. Am J Clin Oncol 35: 399-405, 2012.
27. Kidd EA, Spencer CR, Huettner PC, Siegel BA, Dehdashti F, Rader JS and Grigsby PW: Cervical cancer histology and tumor differentiation affect ^{18}F-fluorodeoxyglucose uptake. Cancer 115: 3548-3554, 2009.

28. Singh N and Arif S: Histopathologic parameters of prognosis in cervical cancer-a review. Int J Gynecol Cancer 14: 741-750, 2004.
29. Razek AA and Nada N: Correlation of choline/creatine and apparent diffusion coefficient values with the prognostic parameters of head and neck squamous cell carcinoma. NMR Biomed 29: 483-489, 2016.
30. Jung NY, Kim SH, Kang BJ, Park SY and Chung MH: The value of primary tumor (18)F-FDG uptake on preoperative PET/CT for predicting intratumoral lymphatic invasion and axillary nodal metastasis. Breast Cancer 23: 712-717, 2016.
31. Monteil J, Maubon A, Leobon S, Roux S, Marin B, Renaudie J, Genet D, Fermeaux V, Aubard Y and Tubiana-Mathieu N: Lymph node assessment with ^{18}F-FDG-PET and MRI in uterine cervical cancer. Anticancer Res 31: 3865-3871 2011.
32. Chen YB, Liao J, Xie R, Chen GL and Chen G: Discrimination of metastatic from hyperplastic pelvic lymph nodes in patients with cervical cancer by diffusion-weighted magnetic resonance imaging. Abdom Imaging 36: 102-109, 2011.
33. Sala E, Rockall AG, Freeman SJ, Mitchell DG and Reinhold C: The added role of MR imaging in treatment stratification of patients with gynecologic malignancies: What the radiologist needs to know. Radiology 266: 717-740, 2013.

This work is licensed under a Creative Commons Attribution-NonCommercial-NoDerivatives 4.0 International (CC BY-NC-ND 4.0) License.